Long-range effects on the periodic deformable sine-Gordon chains

1999 J. Phys.: Condens. Matter 11 L75

(http://iopscience.iop.org/0953-8984/11/11/001)

J. Phys.: Condens. Matter **11** (1999) L75–L81. Printed in the UK PII: S0953-8984(99)98517-X

LETTER TO THE EDITOR

Long-range effects on the periodic deformable sine–Gordon chains*

David Yemélé† and Timoléon C Kofané†‡

† Laboratoire de Mécanique, Faculté des Sciences, Université de Yaoundé I, BP 812 Yaoundé, Cameroun

‡ Laboratoire de Physique de l'Université de Bourgogne, avenue Alain Savary, BP 400, 21011 Dijon, France

Received 20 October 1998, in final form 26 January 1999

Abstract. The model of long-range interatomic interactions is found to reveal a number of new features, closely connected with the substrate potential shape parameter s. The phase trajectories, as well as an analytical analysis, provide information on a disintegration of solitons upon reaching some critical values of the lattice parameters. An implicit form for two classes of these topological solitons (kink) is calculated exactly.

In the last few years, a great amount of attention has been devoted to the dynamics and thermodynamics of the nonlinear one-dimensional (1D) lattices with long-range interaction (LRI) potential [1–8]. This attention has been motivated by the fact that, in real materials, the interactions between particles are more complicated and extend further than the nearest-neighbour interactions, for instance, in ferroelectric chains and in adsorption systems where adatomic charges create coulomb repulsion forces, dipole–dipole interaction and direct or indirect interaction [7]. Also, it is an alternative approach to treat the problem of phase transition in most of the condensed matter systems besides the approach which consists of considering the two- or three-dimensional nature of the system [1].

Among the various types of LRI potential (power-law interaction [3, 7], Lennard-Jones long-range coupling [2] and exponential interaction such as Kac–Baker potential [8]), a well studied example is the Kac–Baker LRIs in which the interaction between particles falls off exponentially as the separation distance between them increases. However, the rigorous applicability remains limited, since it is unlikely that real physical condensed matter systems will be 'exactly' described by potentials with defined shapes [1, 4]. All these studies ignored the fact that the shape of the nonlinear one-site potential may deviate considerably from that attributed to the local potential. For example, in H/W (hydrogen atoms adsorbed on a tungsten surface), the shape of the substrate potential deviates from the sine–Gordon (sG) potential [7].

It is the main purpose of this letter to present briefly the results concerning two classes of implicit form of topological or kink solitons in the Remoissenet–Peyrard (RP) model [9] with the Kac–Baker LRI potential. We demonstrate that the competition between the shape s and long-range parameters r leads to some qualitatively new effects. Among these effects, absent from the sG model with the Kac–Baker LRIs [4], one should note the disintegration of the

* This letter is dedicated to Professor M Remoissenet on the occasion of his 65th birthday.

0953-8984/99/110075+07$19.50

solitons for 'effective substrate potential amplitudes', exceeding some critical threshold value, as well as the dependence on s of these nonlinear excitations.

We consider a system of ions of mass m placed in an infinite 1D lattice of spacing b. The Hamiltonian is given by

$$H = \sum_i (m/2)\dot{u}_i^2 + \sum_i \sum_{j \neq i} (V_{ij}/2)(u_i - u_j)^2 + \sum_i V_0 V_{RP}(2\pi u_i/a_s, s) \qquad (1)$$

where u_i and $\dot{u}_i$ denote the position and the velocity of the ith ion, respectively a_s and V_0 are respectively the period and the amplitude of the substrate potential. The ith ion and jth ion are assumed to interact harmonically with elastic coupling constant coefficient V_{ij} of the Kac–Baker form $V_{ij} = [C(1-r)/2r]r^{|i-j|}$, where $|i-j|$ measures the absolute distance between the two sites i and j and the parameters r and C are respectively the range of interactions with $0 \leqslant r < 1$ and the elastic constant of the lattice. For a given r, V_{ij} decreases when j increases. Experimentally, one can relate the parameter r to the number of neighbouring interactions. Note that the limit $r \to 0$ reduces to the nearest-neighbour problem and the limit $r \to 1$ defines the infinite-range problem. In the latter case, also known as the Van der Waals limit, the system may exhibit a phase transition at a finite temperature [1]. We focus our attention on the one-site RP potential [9]

$$V_{RP}(2\pi u_i/a_s, s) = (1-s)^2 \frac{1 - \cos(2\pi u_i/a_s)}{1 + s^2 + 2s\cos(2\pi u_i/a_s)} \qquad |s| < 1 \qquad (2)$$

where s is the shape parameter. This potential reduces to the sG potential in the limit of $s \to 0$. In the adsorption system, the expression of a frequency of oscillations of an isolated particle at the bottom of the substrate potential is $\omega_s = \omega_0(1-s)/(1+s)$, where $\omega_0 = (2\pi/a_s)(V_0/m)^{1/2}$. With the help of the expression for ω_s, it is more reliable to determine the parameter s directly from experimental data using the measured values of V_0 (activation energy of a particle), a_s, m and ω_s. Estimates for e.g. H/W and Li/W adsystems yield -0.3 and -0.2, respectively. For the sake of simplicity, we define the quantities $M = m(a_s/2\pi)^2$, $k = C(a_s/2\pi)^2$ and the dimensionless displacement $\theta_i = 2\pi u_i/a_s$, so that the Hamiltonian (1) can be rewritten as

$$H = \sum_i \frac{1}{2} M\dot{\theta}_i^2 + \sum_i \sum_{j \neq i} \frac{k(1-r)}{2r} r^{|i-j|}(\theta_i - \theta_j)^2 + \sum_i V_0 V_{RP}(\theta_i, s). \qquad (3)$$

The equation of motion for θ_i which follows from (3) is

$$M\ddot{\theta}_i + V_0\,\mathrm{d}V_{RP}(\theta_i, s)/\,\mathrm{d}\theta_i + 2k\theta_i = L_i \qquad L_i = \frac{k(1-r)}{r} \sum_{j \neq i} r^{|i-j|\theta_j} \qquad (4)$$

where the auxiliary quantity L_i satisfies the recursion relation

$$L_{i+1} + L_{i-1} = (r + (1/r))L_i - \frac{k(1-r)}{r}(\theta_{i+1} + \theta_{i-1} - 2\theta_i). \qquad (5)$$

Now, we go to the continuum limit, where the approximation $\theta_i(t) \to \theta(x,t)$ and $L_i(t) \to L(x,t)$ can be used with $x = ib$. A Taylor expansion of variables with indices $i+1$ and $i-1$ around variables of index i, to the second order, transforms equation (5) into the nonlinear partial equation. When we look for solutions in the form of travelling waves $\theta(x,t) = \theta(x - vt)$ with constant velocity v, it reduces to

$$\theta_{yy} + \sigma(r)(V'_{RP}(\theta, s))_{yy} = V'_{RP}(\theta, s) \qquad (6)$$

with $y = (x - vt)/\xi(r)$, where

$$\xi(r)^2 = \xi_0^2(r)[1 - (v^2/C_0^2(r))] \qquad \sigma(r) = \sigma_0(r)/[1 - (v^2/C_0^2(r))]. \qquad (7)$$

with

$$\sigma_0 = V_0/k \qquad \xi_0^2 = kb^2/V_0 \qquad C_0^2 = kb^2/M$$
$$\sigma_0(r) = \sigma_0 r/(1+r) \qquad \xi_0^2(r) = \xi_0^2(1+r)/(1-r)^2 \qquad C_0^2(r) = C_0^2(1+r)/(1-r)^2. \tag{8}$$

The subscripts y and the prime stand for the derivative with respect to y and θ, respectively. The LRI dependent parameter $\sigma(r)$ plays the role of an 'effective substrate potential amplitude' while $\xi_0(r)$ and $C_0(r)$ are the characteristic length of the system and the sound velocity, respectively. The solutions of equation (6) can be best analysed in the phase plane (θ, θ_y). Thus, this equation can be treated as an autonomous dynamic system where the first integral is given by

$$\theta_y^2 = \frac{2V_{RP}(\theta, s) + \sigma(r)[V'_{RP}(\theta, s)]^2 + \tilde{K}}{(1 + \sigma(r)V''_{RP}(\theta, s))^2} \tag{9}$$

where $\tilde{K}$ is an integration constant. It is clear from equation (9) that the system exhibits two equilibrium points $(\theta, \theta_y) = (0, 0)$ and $(\pi, 0)$ characteristic for the classical sG systems. Figure 1 shows the phase trajectories of the system for three fundamental types of result. In figure 1(a), one encounters the classical closed ($\tilde{K} < 0$) and open ($\tilde{K} > 0$) trajectories corresponding to periodic waves of constant sign (nonlinear oscillations in the potential well) and alternating-sign periodic waves. The separatrix ($\tilde{K} = 0$) with corresponds to a single soliton is a solid line for all $\theta \in [0, 4\pi]$.

When $\sigma(r)$ increases upon reaching some critical value σ_c, the phase portrait changes qualitatively. The two fixed points are still present but one encounters the close trajectories around π where the amplitude is limited by the singular points θ_{s2} (see figure 1(b)). In the case $s > 0$, this motion is reduced to a fixed point $(\pi, 0)$ corresponding to a potential well. In both cases ($s > 0$ and $s < 0$), we notice the absence of the separatrix indicating the breakdown of the solitons. This situation is justified by the existence of the singular points in the vicinity of which θ_y tends to infinity. The exact position of these new special points may be derived from the singularity arising in the denominator of equation (9). Evidently, their existence causes the destruction of the solitons. It should disappear if the effective depth of the substrate potential is $\sigma(r) < \sigma_c$, with

$$\sigma_c = -\frac{(\alpha^2 + \gamma^2)}{\alpha^2(1 + \gamma^2)}(\alpha^2 + 3(\alpha^2 - 1)\gamma^2 - \gamma^4) \text{ for } s < 0 \qquad \sigma_c = \alpha^2 \text{ for } s > 0 \tag{10a}$$

where

$$\gamma^2 = \frac{(3 - 8\alpha^2 + 3\alpha^4) + (9\alpha^8 - 24\alpha^6 + 30\alpha^4 - 24\alpha^2 + 9)^{1/2}}{2(3\alpha^2 - 2)} \qquad \alpha = (1 - |s|)/(1 + |s|). \tag{10b}$$

Figure 2 shows the variation of σ_c with the deformable parameter s. Below the critical value σ_c ($0 \leqslant \sigma(r) \leqslant \sigma_c$), corresponding to area I, a kink exists, and above this value (area II) no kinks whatsoever may exist. Also, for each value of ξ_0, r, there exists a boundary in the v and s plane and trespassing over this boundary causes the destruction of the solitons since, from equation (10), the limiting value v_c of the kink velocity is $v_c = C_0(r)(1 - \sigma(r)/\sigma_c)^{1/2}$. For example for $\sigma_0 \simeq 1$ and $r = 0.1$, $v_c \simeq 0.3C_0$ for $s = 0.5$ and $v_c \simeq 0.01C_0$ for $s = 0.6$. This means that for $|s| < 0.6$ no kinks may exist even at very low velocity.

Following the preceding investigations, for $\sigma(r) < \sigma_c$, the system exhibits soliton solutions. Now, we confine our attention to the case $\tilde{K} = 0$ which describes solitons which play an important role in the dynamics of the system. The solutions which correspond to

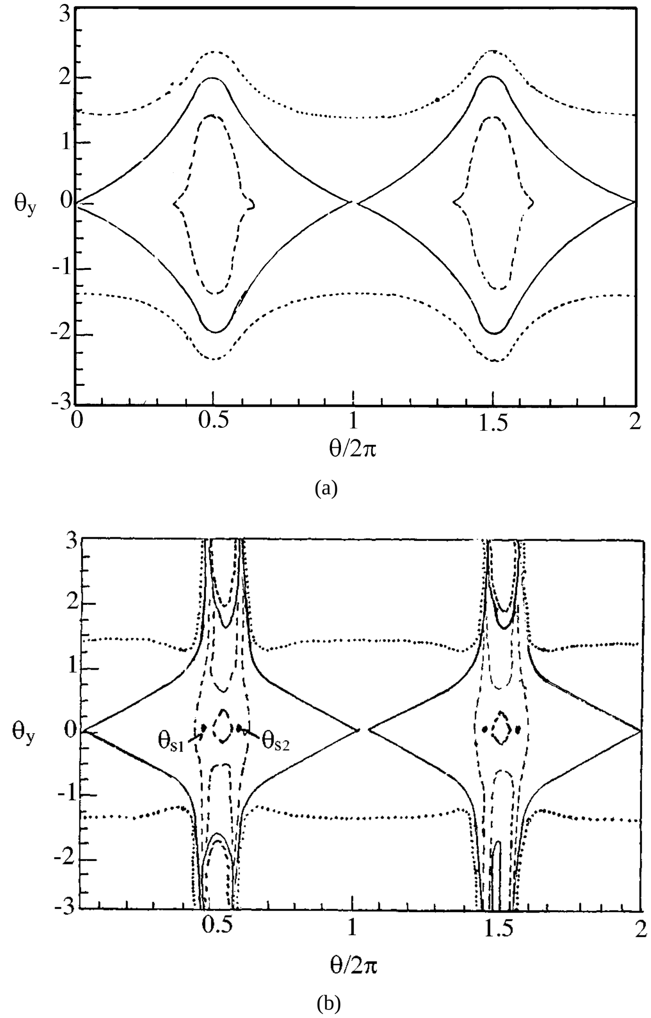

Figure 1. Phase trajectories in two periods of the substrate potential for the deformable parameters $s = -0.5$ for (a) $\sigma(r) = 0$ and (b) $\sigma(r) = 0.1$, in units $\theta/2\pi$, according to equation (9).

kinks verify the following classical boundary conditions: $\theta_y \to 0, \theta \to (2\pi, 0)$ as $y \to \pm\infty$. Then, from equation (9) one can obtain after some lengthy algebra two families of implicit kink solutions

$$\begin{aligned}(Z_1 - Z_2)^{1/2}(y - y_0) = \operatorname{sgn}(\theta - \pi)\{&[D_1 + (A_1/Z_3) + (B_1/(1 + Z_3)) \\ &+(C_1/(\alpha^2 + Z_3))]F(\nu, q) - [(A_1/Z_3)\pi(\nu, -Z_3/(Z_1 - Z_3), q) \\ &+(B_1/(1 + Z_3))\pi(\nu, (-1 - Z_3)/(Z_1 - Z_3), q) \\ &+(C_1/(\alpha^2 + Z_3))\pi(\nu, (-\alpha^2 - Z_3)/(Z_1 - Z_3), q)]\}\end{aligned} \tag{11a}$$

for $-1 < s \leqslant 0$ and

$$\begin{aligned}(Z_1' - Z_2')^{1/2}\alpha^4(y - y_0) = \operatorname{sgn}(\theta - \pi)\{&[D_1' + (A_1'/Z_3') + (B_1'/(1 + Z_3')) \\ &+(C_1'/(1 + \alpha^2 Z_3'))]F(\mu, p) - [(A_1'/Z_3')\pi(\mu, -Z_3'/(Z_1' - Z_3'), p) \\ &+(B_1'/(1 + Z_3'))\pi(\mu, (-1 - Z_3')/(Z_1' - Z_3'), p)\end{aligned}$$

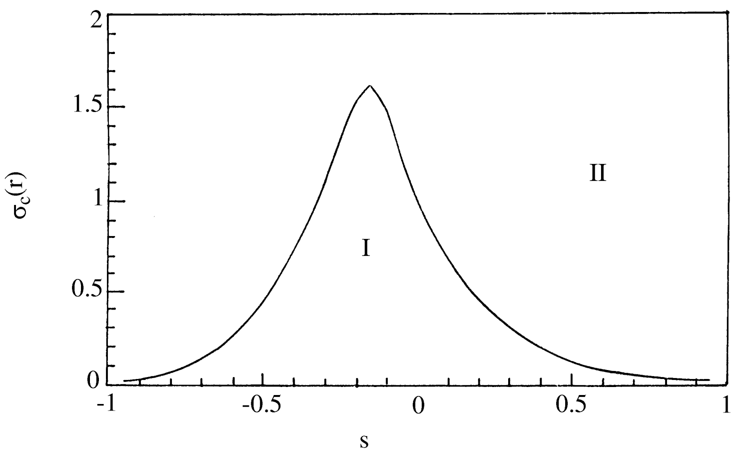

Figure 2. Variation of the critical effective substrate potential amplitude as a function of the deformable parameter s.

$$+(C_1'/(1+\alpha^2 Z_3'))\pi(\mu, (-1-\alpha^2 Z_3')/(Z_1'-Z_3'), p)]\} \tag{11b}$$

for $0 \leqslant s < 1$, with

$$\nu = \tan^{-1}((Z_1 - Z_3)/(\tan^2(\theta/2) - Z_1))^{1/2} \qquad q = ((Z_2 - Z_3)/(Z_1 - Z_3))^{1/2}$$
$$A_1 = \alpha^2(\sigma(r) + \alpha^2) \qquad B_1 = -(1-\alpha^2)^2 \qquad C_1 = -4\alpha^2\sigma(r)(1-\alpha^2)$$
$$D_1 = 1 - \alpha^2\sigma(r) \tag{12a}$$

and

$$\mu = \tan^{-1}((Z_1' - Z_3')/(\tan^2(\theta/2) - Z_1'))^{1/2} \qquad p = ((Z_2' - Z_3')/(Z_1' - Z_3'))^{1/2}$$
$$A_1' = (1 + \alpha^2\sigma(r)) \qquad B_1' = -(1-\alpha^2)^2 \qquad C_1' = 4\alpha^2\sigma(r)(1-\alpha^2)$$
$$D_1' = \alpha^4(\alpha^2 - \sigma(r)) \tag{12b}$$

where F and π are the first and third elliptic integrals, respectively and Z_1, Z_2 and Z_3 verify the following equation

$$Z^3 + \alpha^2(3 + \sigma(r)\alpha^2)Z^2 + \alpha^4(3 + 2\sigma(r))Z + \alpha^4(\alpha^2 + \sigma(r)) = 0$$

while Z_1', Z_2' and Z_3' verify

$$\alpha^6 Z^3 + \alpha^2(3\alpha^2 + \sigma(r))Z^2 + \alpha^2(3 + 2\sigma(r))Z + (1 + \alpha^2\sigma(r)) = 0.$$

Note that $Z_1 > Z_2 > Z_3$ and $Z_1' > Z_2' > Z_3'$. The antikink solutions are obtained by replacing θ by $(2\pi - \theta)$ in equations (11) and (12). As $r \to 0$ ($\sigma(r) \to 0$), equations (11a) and (11b) reduce to the form of the RP soliton [9] while as $s \to 0$ they reduce to the sG kink with LRIs [4].

From equation (9) the spatial extension of the kink (pseudo-kink width) is given by

$$L_k = \xi(r)\alpha/(1 + \sigma(r)\alpha^2)^{1/2} \text{ for } -1 < s \leqslant 0$$
$$L_k = \xi(r)/(\alpha^2 + \sigma(r))^{1/2} \text{ for } 0 \leqslant s < 1. \tag{13}$$

As $r \to 0$, L_k reduces to $L_k = \xi_0\alpha$ for $-1 < s \leqslant 0$ and $L_k = \xi_0/\alpha$ for $0 \leqslant s < 1$. For $s < 0$, this width increases with r for all values of s and slightly decreases in the range $0 \leqslant r \leqslant 0.2$ for $s > 0$, and the soliton slowly disappears as $r \to 1$. This is shown in figure 3(a) where θ is

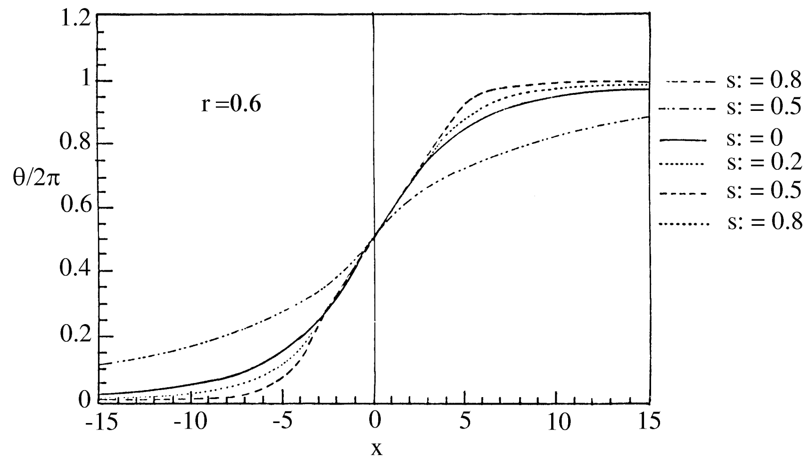

(a)

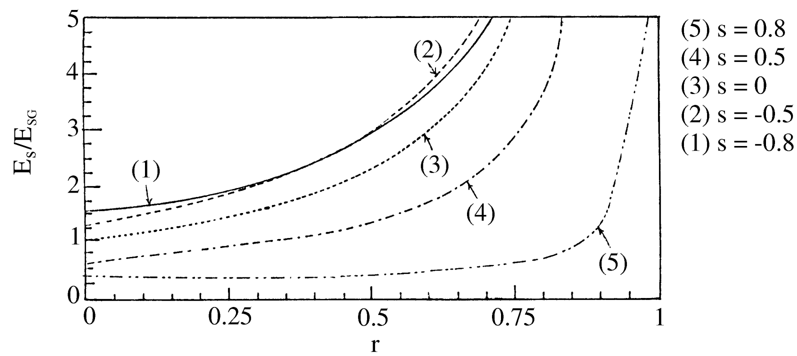

(b)

Figure 3. (a) The soliton profile $\theta(y/\xi_0)$ for various values of the shape parameter s. (b) The soliton creation energy, plotted in units of the sG soliton energy $E_{sG} = 8b(kV_0)^{1/2}$, versus r, for a few s.

plotted against y (with $v = 0$) for various values of the LRIs' parameter r and the deformable parameter s.

We now look for the calculation of the soliton energy. For this aim, we use the auxiliary quantity L_i and equation (3) and go to the continuum limit. Then, using equation (9), the total energy of the system (soliton energy) can be written in the more suggestive form as

$$E_s = E_p + E_k = I_1(2Mv^2 + \xi^2(r)V_0)/(2b\xi(r)) + I_2\sigma(r)\xi(r)V_0/2b + I_3V_0\xi(r)/b \tag{14}$$

with

$$I_1 = \int_0^{2\pi} \mathrm{d}\theta(2V_{RP}(\theta, s) + \sigma(r)[V'_{RP}(\theta, s)]^2)^{1/2}(1 + \sigma(r)V''_{RP}(\theta, s))^{-1}$$

$$I_2 = \int_0^{2\pi} \mathrm{d}\theta V''_{RP}(\theta, s)(2V_{RP}(\theta, s) + \sigma(r)[V'_{RP}(\theta, s)]^2)^{1/2}(1 + \sigma(r)V''_{RP}(\theta, s))^{-1} \tag{15}$$

$$I_3 = \int_0^{2\pi} \mathrm{d}\theta V_{RP}(\theta, s)(1 + \sigma(r)V''_{RP}(\theta, s))(2V_{RP}(\theta, s) + \sigma(r)[V'_{RP}(\theta, s)]^2)^{-1/2}$$

where we have made use of the fact that $y(+\infty) = 2\pi$ and $y(-\infty) = 0$. The first obvious remark is that the integrals I_1, I_2 and I_3 are analytically intractable for the potential $V_{RP}(\theta, s)$. However in the limit $s \to 0$ (sG potential), the calculation is possible and reduces to that obtained in the sG potential with LRIs [4]. To find the energy of the soliton in the whole range of interaction $0 \leqslant r < 1$ and for all values of the deformable parameter $-1 < s < 1$, we have integrated equation (15) numerically. The results are shown in figure 3(b) for a few values of the deformable parameter. It is seen that E_s is an increasing function of the range of interaction for all values of s. In the limit $r \to 1$, E_s goes to infinity. It seems very likely that this state is energetically less favourable for the existence of the soliton since all the particles sit at the top of the potential well. Note that, in this model, three facts contribute to lower the kink energy: first, an increase in the coupling ($\sigma_0 \ll 1$); second, a potential with a sufficiently flat bottom ($s \to 1$), like an RP system, and third a decrease in the long-range parameter. Nevertheless, the two first cases correspond to very large kinks. Since E_s corresponds to the energy of creation of the soliton, this result suggests that, physically, kinks would be more easily created in systems where the potentials have flat bottoms ($s > 0$) and small LRIs.

In this paper the RP model with long-range effect interactions between the ions of the chain is shown to give some qualitatively new results arising from the deformability of the substrate potential shape, such as the appearance of a new type of phase trajectory and the breakdown of conventional solitons. Also, another effect is related to a transition from open to closed phase trajectories of the system taking place beyond some threshold values of the lattice parameters and/or the velocity of the soliton propagation. An exact analytical expression for the dependence of the breakdown threshold value on the shape parameter of the RP potential, on the LRIs' parameter and on the velocity of the kinks has been derived. It is shown that these new features stem from the deformability of the shape of the substrate potential and, therefore, that they should be encountered in real systems. Our analysis shows that the shape of the substrate potential is of great importance for modelling nonlinear systems particularly when the LRIs are involved. Thermodynamic and transport properties of the model, which is the extension of the short-range model [10, 11], are now in progress and the results will be presented in the near future.

References

[1] Saker S K and Krumhansl J A 1981 *Phys. Rev.* B **23** 2374
[2] Ishimori Y 1982 *Prog. Theor. Phys.* **68** 402
[3] Pokrovsky V L and Virosztek A 1983 *J. Phys. C: Solid State Phys.* **16** 4513
[4] Woafo P, Kenné J R and Kofané T C 1993 *J. Phys.: Condens. Matter* **5** L123
Woafo P, Kenné J R and Kofané T C 1994 *J. Phys.: Condens. Matter* **6** 4277
[5] Vasquez L, Evans W A B and Rickayzen G 1994 *Phys. Lett.* A **189** 454
[6] Gaididei Y, Flytzanis N, Neuper A and Mertens F G 1995 *Phys. Rev. Lett.* **75** 2240
[7] Braun O M, Kivshar Y S and Zelenskaya H 1990 *Phys. Rev.* B **41** 7118
[8] Baker G A Jr 1961 *Phys. Rev.* **122** 1477
Kac M and Helfand E 1973 *J. Math. Phys.* **4** 1078
[9] Remoissenet M and Peyrard M 1981 *J. Phys. C: Solid State Phys.* **14** L481
[10] Yemélé D and Kofané T C 1997 *Phys. Rev.* E **56** 1037
[11] Yemélé D and Kofané T C 1997 *Phys. Rev.* B **56** 3353